

**Title:**

“Development of an AYUSH-based synergistic combination against *Mycobacterium avium* subspecies *paratuberculosis* - A major disease liability of the dairy industry”

**Introduction:**

The synergistic approach in herbal medicine is being employed as a tool for research ideas. Herbal medicine's uniqueness is due to presence of multiple phytoconstituents and interactions (synergistic, additive or antagonistic) between constituents. It has been noted that, despite widespread interest in synergy and its importance in herbal therapy, it is not widely documented or written about. Identifying the pharmacological mechanisms of herbal remedies provides distinct challenges in research than that of synthetic pharmaceuticals (Patwardhan and Mashelkar, 2009).

Crohn's disease, a potential inflammatory bowel disorder is similar to some aspects of leprosy, tuberculosis and paratuberculosis. Some studies reported in reputed journals state the presence of viable MAP bacilli in individuals with Crohn's disease. Controlling MAP is challenging since bacilli are passed on to the next generation via sperm, pregnancy, through colostrum and milk feeding. As a result, the transmission of MAP to the next generation cannot be prevented. Vaccination and 'test and cull' approaches are used globally to control disease and stop transmission in animals. However, due to the absence of vaccine, MAP infection in humans can be controlled either by surgical removal of diseased intestines or by anti-tuberculosis treatments, with limited efficacy. Prolonged usage of known anti-tuberculosis medications result in drug resistance (Azagra-Boronat et al., 2020).

Hence, there exists a need to develop alternatives against this infection. *Ocimum sanctum* Linn and *Solanum xanthocarpum* Schrad & Wendl are reported to have anti-inflammatory and immunomodulatory potential in the ancient system of medicine (Goel et al., 2010; Kajaria et al., 2013). Herb-integrated synergistic approach has never been explored earlier against this infection. This novel initiative is a promising step towards the development of efficient alternatives for the management of such infection. Transmission and pathogenesis of *Mycobacterium avium* subspecies *paratuberculosis* (MAP) infection is depicted in **Fig. 1**.

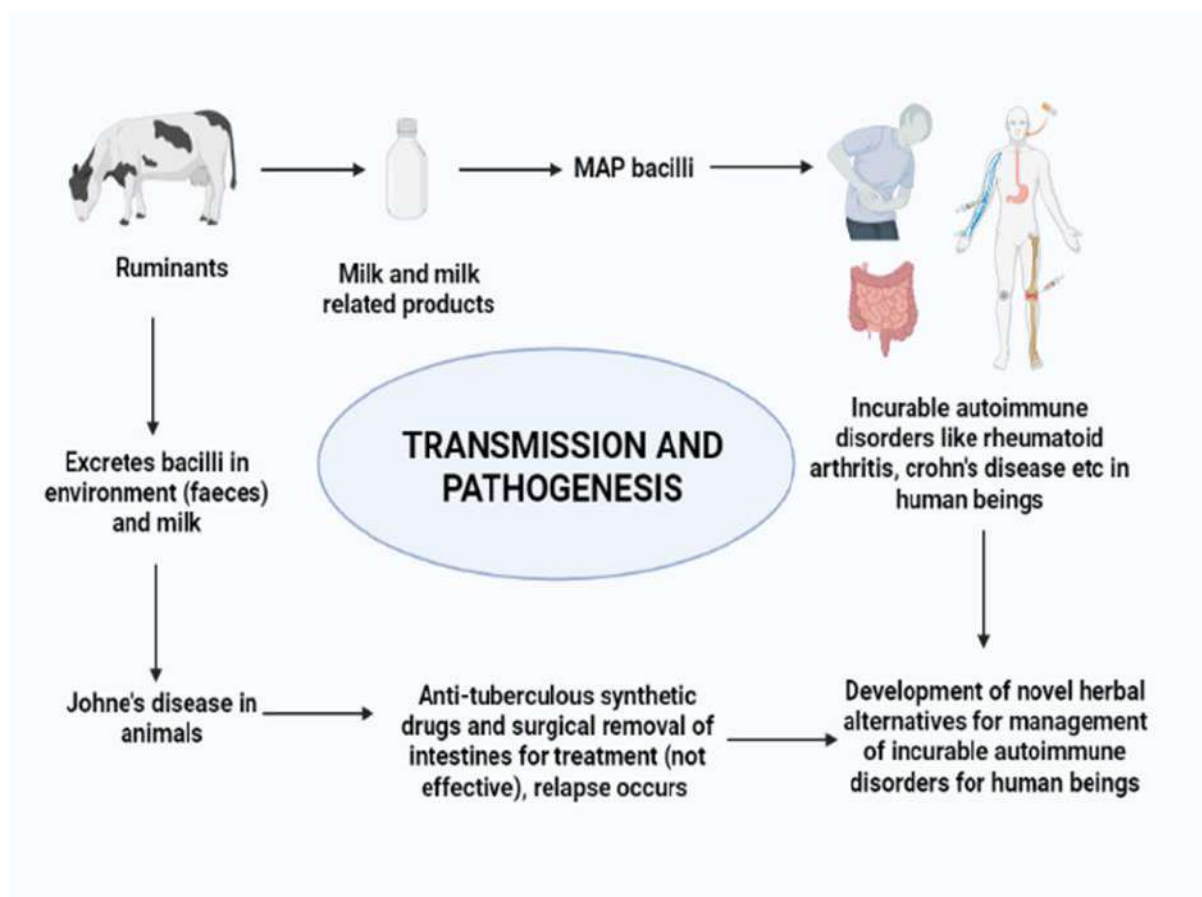


**Figure 1: Transmission and pathogenesis of *Mycobacterium avium* subspecies *paratuberculosis* (MAP) infection**

### Objectives

- Procurement, authentication and preparation of aqueous, ethanolic and hydroethanolic extracts of selected plants.
- *In vitro* analysis for selection of Best Bioactives (BAEs) for preparation of Synergy-based formulation (SBF).
- Quality control and metabolomic analysis
- *In vivo* immunomodulatory, acute toxicity, pharmacokinetics and pattern recognition analysis of SBF.

### Materials and Methods

#### **Objective 1: Procurement, authentication and preparation of aqueous, ethanolic and hydroethanolic extracts of selected plants.**

The respective parts of the plants will be collected freshly just before initiation of the experiment and authenticated using botanical and phytochemical standards. Further these will be deposited in laboratory with our specimen number for future use.

Plant samples will be washed under running tap water to remove any type of contamination and air-dried at room temperature to remove moisture and stored in air-tight container prior to the extraction. The dried plant parts will be powdered and extracted by using suitable solvents including aqueous, ethanolic and hydro ethanolic by using suitable extraction methods to get three extracts of each plant. The obtained extracts will be used for *invitro* studies to find out two best active extracts. Further, both the extracts will be used to prepare the formulation (AYUSH model).

**Objective 2: *In vitro* analysis for selection of Best Bioactives (BAEs) for preparation of Synergy-based formulation (SBF).**

Anti-mycobacterial activity of the plant extracts will be conducted using BACTEC MGIT 960 liquid culture method and Resazurin Microtiter Assay (REMA). Briefly, MAP culture will be incubated with different concentrations extracts and fractions ranging from 10-200 µg/mL anti-MAP drugs for 5 days in REMA, and for 2 weeks in MGIT 960system (Schena et al., 2016).

Comparative evaluation of pharmacological properties along with inhibitory effects of the selected plant extracts with anti-MAP drug combinations (first line of anti-mycobacterial drugs) by *invitro* culture sensitivity test.

Fractional inhibitory concentration (FIC) index will be calculated as per the reported protocol (Van Vuuren and Viljoen, 2011).

**Objective 3: Quality control and metabolomic analysis**

Quality control of developed formulation as well as best active fractions of each plants will be performed by utilizing different high throughput screening such as HPTLC/HPLC/LCMS (Khan et al. 2017, Zahiruddin et al. 2016).

**Objective 4: *In vivo* immunomodulatory, acute toxicity, pharmacokinetics and pattern recognition analysis of SBF:**

Dosing plan of *in vivo* studies is depicted in Fig. 2.

Group	Description	Route	No. of animals
Group-I	Normal control (Saline)	p.o	3
Group-II	Negative Control (Cyclophosphamide: 80 mg/kg)	i.p	3
Group-III	BAE-I + Cyclophosphamide	p.o+i.p	3
Group-IV	BAE-II + Cyclophosphamide	p.o+i.p	3
Group-V	SBF (High Dose) + Cyclophosphamide	p.o+i.p	3
Group-VI	SBC (Medium Dose) + Cyclophosphamide	p.o+i.p	3
Group-VII	SBF (Low Dose) + Cyclophosphamide	p.o+i.p	3
Group-VIII	Positive Control+ Cyclophosphamide	p.o+i.p	3

**Figure 2: Dosing plan of *in vivo* immunomodulatory studies**

The study will be conducted as per reported protocol (Parveen et al., 2021)

Acute toxicity (LD<sub>50</sub>) studies will be performed according to the reported protocol and guidelines for acute toxicity studies (Jayesh et al., 2017).

Developed formulation and best bioactives will be administered through oral route at normalized dose. At 0, 1.5, 2, 4, 8, 12, 24 h following oral administration, the blood samples will be collected from retro orbital vein to normal tubes and centrifuged at 10,000 rpm for 15 minutes to separate serum and stored at -80°C until analysis. Before analysis serum will be processed as per validated protocol. Sample for kinetic analysis will be analyzed through HPLC/LC-MS (Zahiruddin et al., 2016).

Study will be carried out on target-based metabolites present in the formulation and best bioactives by using several modern analytical techniques such as LC-MS/HPLC for its metabolic profiling. High-throughput profiling of metabolic status of blood will be carried out by LC-MS/GC-MS. Results obtained from this study will be compared before and after treatment in all groups (**Khan et al. 2017; Zahiruddin et al. 2016**).

## Results and Discussion

### *Plant Collection, preparation of bioactive extracts and authentication*

Whole plant parts were freshly collected from the farm area of the local Veterinary University, Mathura (Uttar Pradesh, India). The collected plant materials were authenticated in-house according to the Ayurvedic Pharmacopoeia of India (Anonymous, 2010) having voucher

numbers BNPL/JH/2020/24, BNPL/JH/2020/25 for *Ocimum tenuiflorum* L. stem with roots, leaves and BNPL/JH/2020/26, BNPL/JH/2020/27, BNPL/JH/2020/28 and BNPL/JH/2020/29 for *Solanum virginianum* L. stem, leaves, fruits and roots, respectively and the specimens of the same have been deposited in the Bioactive Natural Product Laboratory, Jamia Hamdard, New Delhi for future reference.

### ***Extraction***

Dried plant materials were powdered and extracted using aqueous, ethanolic, and hydro-ethanolic (50:50 ratio) solvents. Aqueous and hydro-ethanolic extracts were prepared using the reflux method, while, ethanolic extracts were prepared using Soxhlet extraction. The % extractive yields of the prepared extracts were obtained as  $20.65 \pm 0.36$ ,  $8.89 \pm 0.31$  and  $18.55 \pm 0.14$  for *O. tenuiflorum* aqueous, ethanolic and hydro-ethanolic extracts respectively whereas  $18.18 \pm 0.13$ ,  $9.79 \pm 0.02$  and  $14.15 \pm 0.02$  for *S. virginianum* aqueous, ethanolic and hydro-ethanolic extracts respectively. The yield of the extracts obtained complied with the API (Ayurvedic Pharmacopoeia of India)(Anonymous, 2010). The aqueous extracts of both plants exhibited high percentage yields compared to the ethanolic and hydro-ethanolic extracts. Comparing aqueous extracts to organic solvents (such as ethanol or methanol), higher yields are frequently obtained. This is because polar substances such as glycosides, phenolic acids, and flavonoids are easily extracted by water while non-polar substances like terpenoids and alkaloids are more easily extracted using ethanol and other organic solvents (Nawaz et al., 2020). Since the yields of aqueous extracts of both plants are comparatively higher, it can be stated that a larger number of polar compounds might be present in the extracts.

### ***Formulation of a solid dosage form and quantitative estimation using High-Performance Thin Layer Chromatography (HPTLC)***

The SBC was formulated as a solid dosage form in the form of tablets using the direct compression method (SBF) (Gallo et al., 2012). Four markers (solasodine, apigenin, diosgenin and betasitosterol) were assessed quantitatively in the BAEs, SBC, and SBF.

### ***Anti-Myco**acterium** activity of bioactive extracts using the Resazurin Microtitre Assay (REMA), selection of BAEs and combination studies***

Due to its slow-growing nature (Fecteau, 2018), culturing of MAP pathogen is difficult in a liquid medium. However, the same objective has been achieved in our previously published study in which we evaluated the anti-MAP potential of *S. virginianum* extracts (Srivastava et al., 2022). This is a noteworthy accomplishment considering the challenges usually involved in cultivating this virus. The REMA (Resazurin Microtiter test) test was used to measure the anti-MAP potential of different plant extracts using an *in vitro* method. The aqueous, ethanolic, and

hydro-ethanolic extracts of *S. virginianum* and *O. tenuiflorum* were tested for their Minimum Inhibitory Concentration (MIC<sub>50</sub>) values. The MIC<sub>50</sub> values for *O. tenuiflorum* were determined to be 1.56, 0.195, and 0.195 mg/mL for the corresponding extracts. Likewise, for *S. virginianum*, the same extracts' MIC<sub>50</sub> values were reported as 3.124, 0.195, and 0.195 mg/mL. The REMA testing findings indicated that the hydro-alcoholic extracts of *S. virginianum* and *O. tenuiflorum* showed the greatest reduction of MAP progression *in vitro*, making them very noteworthy.

It was observed that the hydro-ethanolic extracts of both plants showed the best inhibition of MAP at MIC<sub>50</sub>=0.195 mg/mL each, hence, were selected as the BAEs. The BAEs were then further investigated for combination studies. Of the five combinations, the BAEs at a 1:1 ratio showed the best inhibition at MIC<sub>50</sub>=0.036 mg/mL with a fractional inhibitory concentration index (FICI) of 0.36 exhibiting synergistic effect and was selected as the SBC. A study by Bharath *et al* reported the anti-MAP potential of ursolic acid (12 µg/mL) and solasodine (60 µg/mL) (Navabharath et al., 2023) which are the major components of the studied plants. Hence, it can be concluded that the anti-MAP potential of *O. tenuiflorum* and *S. virginianum* might be due to these biomarkers. However, there might be other compounds as well contributing to the synergistic effect which need further investigation. The obtained results are illustrated in **Fig. 3** and tabulated in **Table 3**. The conducted study opens avenues for alternative therapies against the targeted pathogen. Further studies can be conducted to elucidate the associated mechanisms underlying the specific compounds in the studied extracts.

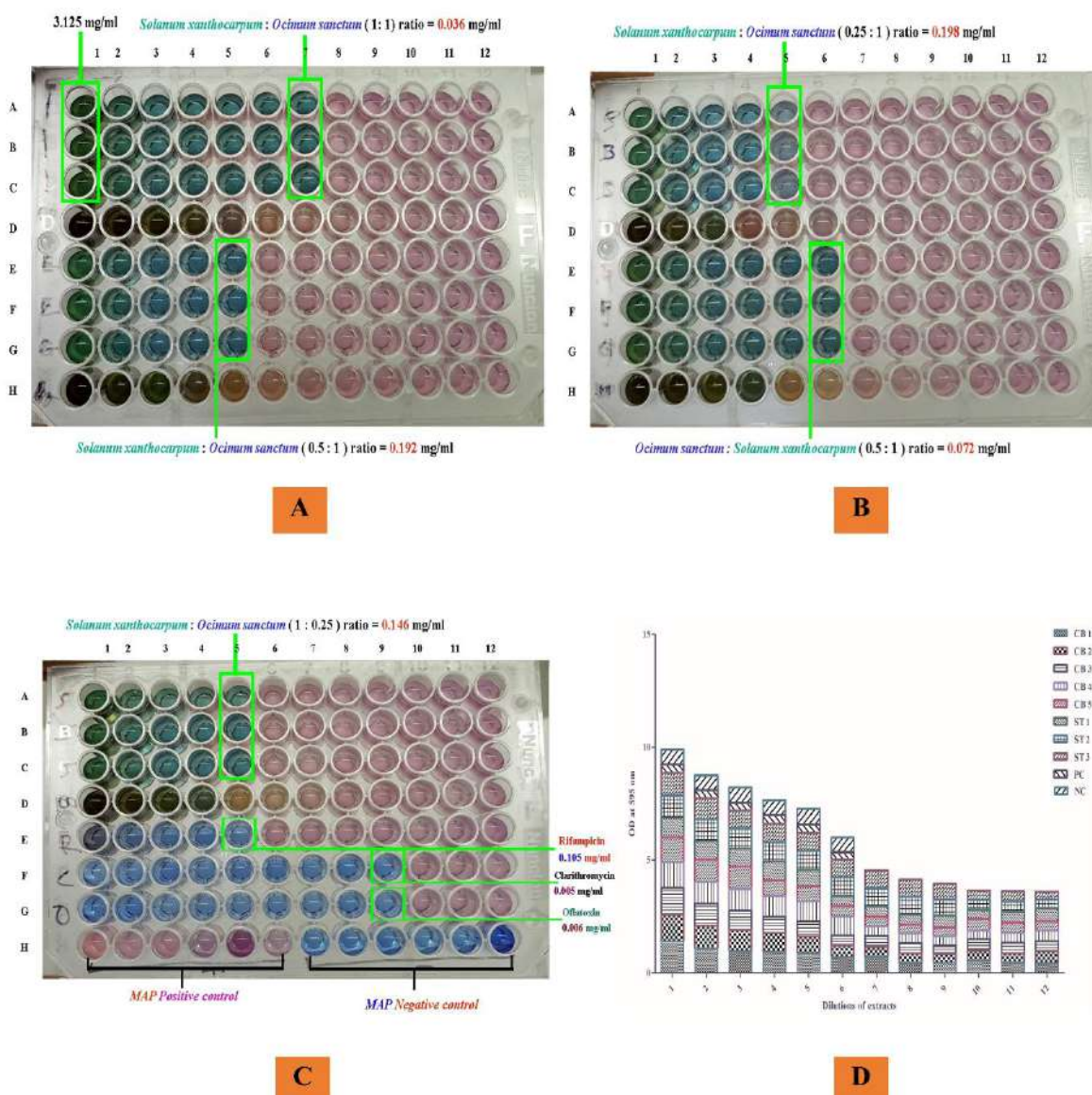


**Fig 3:** *In vitro* REMA assay for determination of best combination ratio. Where, A-C are the illustrations of microtitre plates. (A) 1:1 & 0.5: 1 *Solanum virginianum*: *Ocimum tenuiflorum*); (B) 0.25:1 & 1:0.5 (*Solanum virginianum*: *Ocimum tenuiflorum*); (C) 1:0.25 (*Solanum virginianum*: *Ocimum tenuiflorum*); D: Graphical illustration of combination ratios and control drugs along with observed optical densities at 595 nm.

**Table 3:** Evaluation of anti-MAP activity of BAEs and determination of SBC using the concept of fractional inhibitory concentration index (FICI)

Combination (A: B)	Individual MIC <sub>50</sub> (mg/mL)		MIC <sub>50</sub> in combination (mg/mL)	FICI	Inference
	A	B			
1:1			0.036	0.36	Synergistic



1:0.5	0.195	0.195	0.192	1.96	Indifference
1:0.25			0.198	2.03	Indifference
0.5:1			0.072	0.74	Non-interactive
0.25:1			0.146	1.49	Indifference

### ***Pinocytic Activity Assay***

The immunomodulatory activity of the prepared extracts was assessed *in vitro*, and its action on pinocytes was determined using the pinocytic activity assay. Analysis of pinocytic activity was done via neutral red uptake. The BAEs as well as the SBC were found to have significant immunomodulatory potential. However, the SBC showed comparatively high immunomodulatory effect. The data was statistically assessed using two-way ANOVA and level of significance was determined using Bonferroni posttest using GraphPad Prism software (Version 5.0). At 95% confidence interval,  $P < 0.05$  was considered as statistically significant. Pinocytic activity of BAEs and SBC is depicted in **Fig 4**.

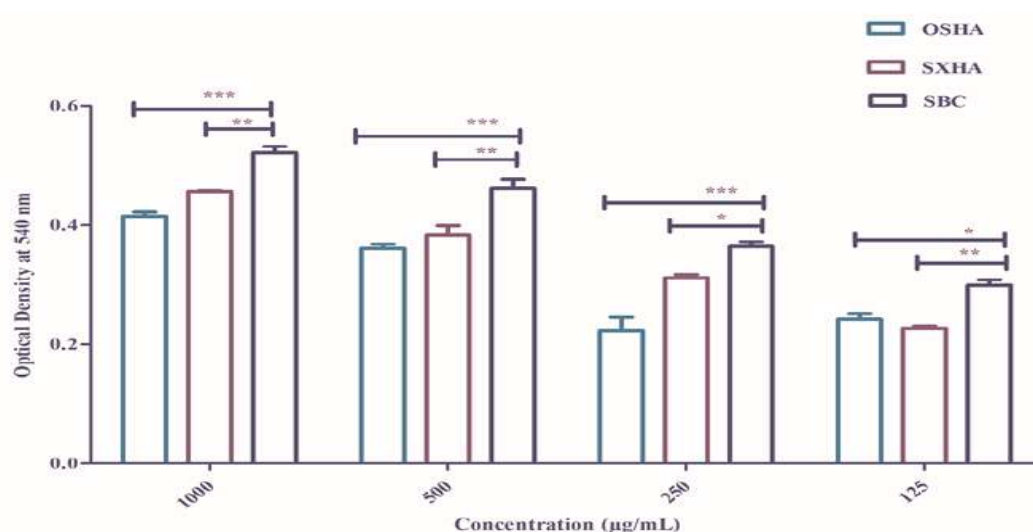


**Fig 4:** The data was statistically assessed using two-way ANOVA and level of significance was determined using Bonferroni posttest using GraphPad Prism software (Version 5.0). At 95% confidence interval,  $P < 0.05$  was considered as statistically significant. Results are depicted as \*\* $P < 0.01$  and \*\*\* $P < 0.001$ . The asterisk “\*” denotes the comparison of data with synergy-based combination.

### ***In vivo studies***



### *Haematological parameters*

#### Hemoglobin (Hb):

A decrease in the hemoglobin levels was observed in the toxic control group administered with cyclophosphamide (Group-II) when compared with the normal control, which indicated anemia. On the other hand, the groups treated with BAE-I + Cyclophosphamide (Group-III), BAE-II + Cyclophosphamide (Group-IV), and SBC (Group-V-VII) restored hemoglobin levels closer to that of the normal control, which may indicate their protective potential against the anemic conditions induced by cyclophosphamide.

#### Neutrophil and Lymphocyte Levels:

The percentage of neutrophils and lymphocytes describes the immune competency with respect to the treatments administered. The number of neutrophils was found to be relatively higher and steady in the different treatment groups compared to the toxic control group. However, the treatments did not have any influence on the level of neutrophils. In the case of the lymphocyte count, it was seen that the count was relatively uniform across the treatment groups, and thus the treatments did not significantly alter the lymphocyte count. However, the neutrophil and lymphocyte levels were larger in the treatment groups that signify slightly enhanced immune response.

#### Total Leukocyte Count (TLC):

TLC represents the total WBC count and reflects the overall immune response of the body. The groups treated with BAE-I + Cyclophosphamide (Group-III), BAE-II + Cyclophosphamide (Group-IV), and SBC (Group-V-VII) at all the treated doses showed TLC closer to the normal control group (Group-I), thus reflecting the possible protective effect against cyclophosphamide-induced leukopenia.

#### Red Blood Cell count (RBC):

It was noted that the toxic control group showed an increase in RBC count compared to the normal control, which might be a compensatory response produced due to decreased hemoglobin levels. Treatment with BAE-I + Cyclophosphamide, BAE-II + Cyclophosphamide, and SBC at all doses brought the RBC close to normal control, thus indicating potential protection against RBC alteration changes induced by cyclophosphamide.

#### Platelet Count:

In contrast, the level of platelets in the negative control group was significantly reduced compared to that in the normal control, an indication of negative control-induced thrombocytopenia. At all screened dose ranges, treatment with BAE-I + Cyclophosphamide, BAE-II + Cyclophosphamide, and SBC showed variable effects on platelet levels, restoring

some doses closer to that of the normal control.

The effects of BAEs and the developed synergistic combination on hematological parameters of wistar rats are tabulated in **Table 4**.

**Table 4: Effect of the anti-MAP synergistic combination on hematological parameters of wistar rats at the end of the treatment**

Haematological parameter	Group-I	Group-II	Group-III	Group-IV	Group-V	Group-VI	Group-VII	Group-VIII
	Normal control (Saline)	Negative Control	BAE-I + Cyclophosphamide	BAE-II + Cyclophosphamide	SBC (High Dose) + Cyclophosphamide	SBC (Medium Dose) + Cyclophosphamide	SBC (Low Dose) + Cyclophosphamide	Positive Control (Levamisole: 10 mg/kg) + Cyclophosphamide
Haemoglobin (gm/dL)	12.8±0.20	10.9±0.10	11.4±0.10	11.23±0.06	14.23±0.06	12.1±0.10	11.13±0.06	11.8±0.17
Neutrophil (%)	12.66±0.57	11±0.91	13.16±0.28	12.06±0.11	14.86±0.23	12.1±0.17	11.43±0.40	14.93±0.11
Lymphocyte (%)	77.66±0.57	74.6±0.52	79.86±0.23	81.2±0.34	82.66±0.80	78.2±0.40	79.03±0.05	75.26±0.46
TLC (/cum m)	5920.33±0.57	5491.33±1.52	6032.66±2.88	5121.33±1.52	6120.33±0.57	5810.66±1.15	5250.66±0.57	5650.66±1.15
RBC	6.38±	6.91±	6.03±0.0	5.83±0.0	6.48±0.0	6.16±0.1	5.92±0.0	5.98±0.0

(millions/cm <sup>3</sup> )	0.0057	0.0057	57	57	057	2	05	05
Platelet count (lakh/cm <sup>3</sup> )	3.91±0.005	4.02	3.26±0.46	1.70±0.005	7.67±0.005	5.50±0.005	4.80±0.05	5.03±0.23

### *Histopathological examination*

#### **Spleen**

In the normal control group, **Fig 6A** the spleen architecture is well-defined and intact. The red pulp appeared of normal and organized structure, maintaining its essential functions and appearance. Central arteries were intact and well structured, indicating a healthy vascular component within the spleen. Marginal zones are clear and distinct, indicating a well-maintained separation between red pulp and white pulp areas. Moreover, follicles F are well-formed and show a typical distribution of lymphocytes, which is an indication of normal immune function and activity within the spleen.

In contrast, the architecture of the spleen in the toxic control group, **Fig 6B** is significantly disturbed. A disruption in the red pulp is noticed with signs of congestion, which may be indicative of impaired blood flow or cellular damage. There was some damage and inflammation to the central arteries, indicating that the toxic agent had some harmful effects on spleen vascular structures. Marginal zones are less distinct, thus proving probable damage, with an impaired separation of the various regions of the spleen. The follicles appear irregular, and the lymphocyte density is reduced, thus showing a defective immune response and altered spleen function.

In the BAE I and BAE II treated groups, **Fig 6C and 6D** the spleen's architecture is appreciably improved compared to the toxic control group. The recovery of red pulp was variable, with some parts showing ample improvement in its structure and organization. Even the central arteries demonstrated recovery in these groups, wherein some of the arteries were near normal in structure, which suggested an appreciative response to the treatment. The marginal zones (MZ) are more defined compared to the toxic control, a finding that suggests partial restituting of the zonal architecture in the spleen. Follicles (F) appear with an improved lymphocyte distribution, suggesting gradual recuperation of immune function.

It demonstrated improvements in low, medium, and high SBC dose groups for different parameters of spleen architecture. RP ranged from mildly to significantly improved in structure, showing dose-dependent character in **Fig 6E-G**. CA demonstrated variable recoveries, some near normal in structure, notably under higher doses. In these treated groups, the marginal zones (MZ) are more defined, which corresponds to an improvement compared with toxic control. The follicles (F) also show a better lymphocyte distribution, and for higher doses, this return to normality is more marked, reflecting an improved immune response.

The spleen in the standard treated group (**Fig 6H**) exhibits the most significant recovery compared to all the treated groups. The structure of red pulp improved much and is near to that of the normal control. The central arteries are very nearly recovered with well-structured intact features. The marginal zones are equally well-marked, thus showing successful restoration of the architecture of the spleen. The follicles (F) are normally structured with normally distributed lymphocytes, showing that immune function has almost returned to normal. This group reflects the efficacy of standard treatment in reducing the toxic effects and regaining the health of the spleen.

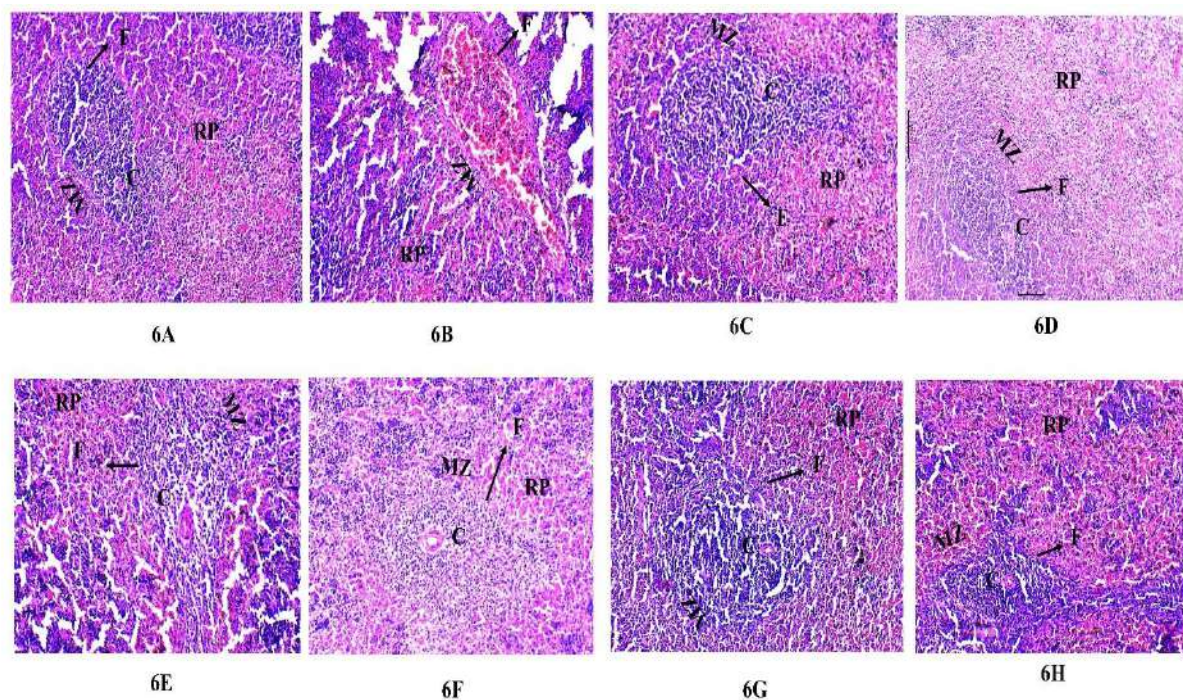


**Fig 6: Histopathological examination of the transverse section of Spleen. Where, RP: Red pulp; C: Central artery; MZ: Marginal Zone and F: Follicle. Where, 6A: Normal Control; 6B: Toxic control; 6C: Treated group (BAE-I); 6D: Treated group (BAE-II); 6E: Treated group (SBC Low dose); 6F: Treated group (SBC Medium dose); 6G: Treated group (SBC High dose) and 6H: Standard control**

## Thymus

The thymic tissue from the normal control group (**Fig 7A**) was quite healthy and harmonious. Lymphocytes were normally distributed and of normal density, showing a good and active immune environment. Hassall's corpuscles were well differentiated and clear in structure with regularity, suggesting a well-preserved thymus architecture. The thymic epithelial cells were normally structured and distributed, further suggesting the absence of any pathologies. The thymic tissue, on the whole, was intact and functioning in the normal control group and this group was utilized as a reference group to compare other experimental groups.

The toxic control groups, **Fig 7B**, however, showed thymic degeneration to a significant level. The number of lymphocytes reduced significantly, many of them showing characteristic signs of apoptosis. Such reduction in the density of lymphocytes would compromise the immune response and the health of the cell. The structures of the Hassall's corpuscles were irregular and less distinctive, undoubtedly showing damage to the structure and possibly an impaired function. The TEC showed damaged and irregularly distributed thymic epithelial cells, which further confirmed the appearance of the thymic tissue in such a compromised state. These observations reveal the thymodegenerative influences of the toxic substance on thymic integrity and function.

Recovery and improvement of thymic tissue health, compared to the toxic control, were observed in all treated groups: BAE I, BAE II, SBC Low, SBC Medium, SBC High, and the standard-treated group (**Fig 7C-H**). There was a general trend toward improving lymphocyte density in the treated groups, with enhancement ranging from mild to significant with different treatments and dosages. Increased lymphocyte density may reflect reversal of the apoptotic effects seen in the toxic control group and thus indicate partial or total restoration of immune function. A very good improvement in the formation and structure of Hassall's corpuscles was observed in all treated groups. The corpuscles became more distinct and regular compared to the toxic control, reflecting recovery in thymic architecture and potential functional restoration. In the treated groups, thymic epithelial cells were better distributed with less damage. This improvement may point to a healing process and hint at the efficacy of treatments in attenuating damage induced by the toxic substance. The above results could be interpreted as meaning that the treatment groups of different degrees all showed some therapeutic effects, some of which had remarkable therapeutic effects on the health of the thymus and the immunocompetence. These findings pointed toward the potential of the tested substances in mitigation of toxic effects and the restoration of thymic integrity.



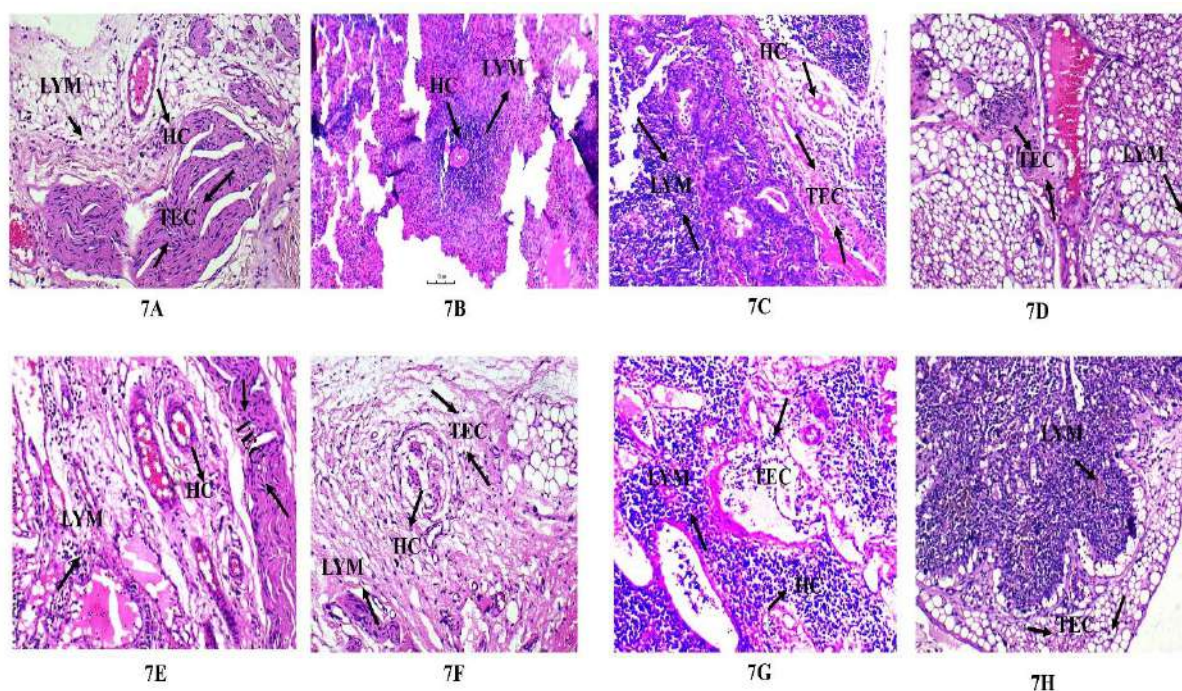


**Fig 7: Histopathological examination of the transverse section of Thymus. Where, LYM: Lymphocytes; HC: Hassall's corpuscles; TEC: Thymic epithelial cells. Where, 7A: Normal Control; 7B: Toxic control; 7C: Treated group (BAE-I); 7D: Treated group (BAE-II); 7E: Treated group (SBC Low dose); 7F: Treated group (SBC Medium dose); 7G: Treated group (SBC High dose) and 7H: Standard control**

#### *Immunohistopathological examination*

##### **Spleen**

The tissue from the normal control group, **Fig 8A** expressed normal levels of CD4 markers, indicating normal populations of T lymphocytes. The immunohistochemical staining was strong and homogeneous, therefore proving the presence of positive cells with CD4, which is an indication of an intact and functional immune response. This identifies, just as expected, the baseline condition of the spleen when it is in a healthy state and hence provides a basis for comparison among other experimental groups.

In contrast, the toxic control group, **Fig 8B** showed lower expression levels of CD4 markers, indicating a drastic reduction in T-lymphocyte populations. Immuno-histo-chemical examination revealed that the number and intensity of CD4-positive cells had dramatically gone down in the immunohistochemistry analysis, thereby pointing out the negative effect of toxicant on the spleen's immunocyte population. Such a decrease in the expression levels of the CD4 markers may indicate the immuno-compromised state of their functioning and hence can be considered as a standard comparison group while testing the efficiency of different

treatments.

Different degrees of improvement in CD4 marker expression levels were seen in the groups treated with BAE I and BAE II (**Fig 8C-D**). In the BAE-I treated spleen tissues, a mild increase in CD4-positive cells was observed, which indicated a slight recovery of T lymphocyte populations. On the other hand, higher CD4 marker expressions were seen in the BAE II treated groups, suggesting a more prominent restorative action on the T lymphocyte populations. These observations suggest that BAE II may be more efficient than BAE I in reverting the toxic agent-induced depletion of immune cells.

Dose-dependent improvements in the marker expression of CD4 were noted in spleen tissues from SBC Low, SBC Medium, and SBC High-treated groups (**Fig 8E-G**). The SBC Low group moderately increased its CD4-positive cells, hence pointing toward the partial recovery of T lymphocyte populations. In relation, the SBC Medium group showed more enhanced expression of CD4, hence indicating substantial restorations into the immune cell population. Among them, the SBC High group was the best and its trend was very close to the normal control group in terms of the level of CD4 marker. Higher dosage SBC treatment was seen to be better in restoring the population of T lymphocytes in the spleen.

In the standard treated group, **Fig 8H** the expression level of CD4 markers was highly improved, representing a robust recovery of the T lymphocyte populations. According to the results of immunohistochemical staining, CD4-positive cells are highly increased, similar to the expression levels exhibited by the normal control group. This finding demonstrates that standard treatment efficiently reverses spleen immune cell population toxicity and could serve as a benchmark in comparing the efficacy of other treatments.

The differences in the degree of restoration of CD4 expression of markers between all the AT-end point treated groups emphasize the possible therapeutic actions of the diverse treatments for replenishment of T lymphocytes, with an illustration of the dose-dependent efficacy very prominent in SBC treated groups. The large relative recovery of the standard treatment group is also a hopeful outcome in which reversal of immune depletion in the spleen is demonstrated, serving as a positive middle dose control group.



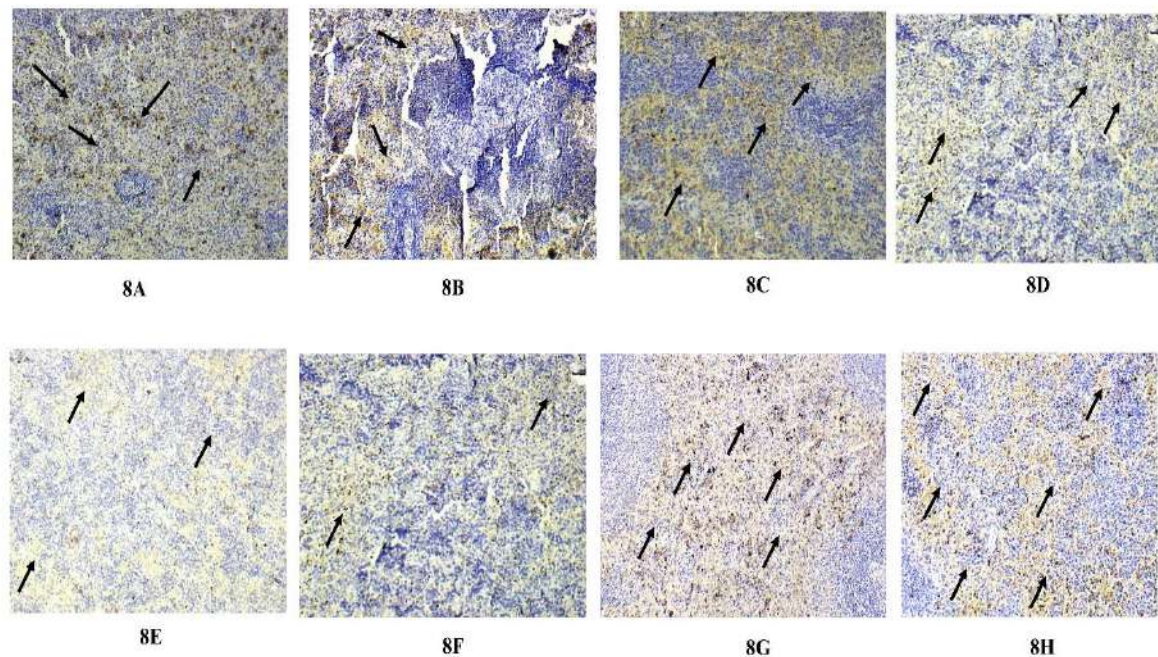


**Fig 8: Immunohistopathological examination of the transverse section of Spleen post-treating with CD4-antibodies. Where the moving arrows signify the produced lymphocytes. Where, 8A: Normal Control; 8B: Toxic control; 8C: Treated group (BAE-I); 8D: Treated group (BAE-II); 8E: Treated group (SBC Low dose); 8F: Treated group (SBC Medium dose); 8G: Treated group (SBC High dose) and 8H: Standard control Thymus**

It showed that the expression levels of the CD4 marker in the normal control group (**Fig 9A**) were within the normal range, thereby pointing toward a healthy population of T-lymphocytes. The tissue of the thymus was a well-structured and proper tissue, showing a dense population of CD4+ cells. This proves the proper functioning of the immune system at work. The results set a base for comparing the effects of various treatments on the expression levels of the CD4 marker.

The expression levels of the CD4 marker in the toxic control group, **Fig 9B** were significantly lowered. The reduction thus indicates a negative effect of exposure to the toxic substance on the immune function by compromising the thymus from maintaining its regular population of T lymphocytes. In the thymus tissue, this group appeared disrupted with few CD4+ cells and much less organized structure compared to the normal control.

The CD4 marker expression levels in treated groups were differently recovered, indicating the restorability in the T-lymphocyte population to some extent.

In the BAE I- and BAE II-treated groups (**Fig 9C-D**), there was a mild to moderate improvement in the expression level of the CD4 marker. This reflected partial recovery of the

T lymphocyte population in the thymus because tissue architecture began to appear very similar to the normal control group with increased cell numbers and more organized aspects of CD4+ cells.

Recovery of CD4 marker expression levels for the SBC Low Treated group (**Fig 9E**) was modest. Though improvement was not high compared to the other groups with higher dosages, a significant hike in CD4+ cells compared to toxic control was nevertheless noted that at lower doses, the treatment had some positive effect on the thymus.

In the SBC Medium treated group **Fig 9F**, there was a significant increase in the expression levels of CD4 marker. Tissue structure of thymus was highly organized and more or less similar to that of the normal control group. An increase in the number of CD4+ cells reflects a significant recovery of the population of T-lymphocyte and hence treatment at this dosage is efficacious.

The SBC High group, **Fig 9G** demonstrated the best recovery in the level of expression of CD4 markers. Actually, thymus tissue expressed almost similarly to the normal control group: a very dense and organized population of CD4+ cells. This means that there is a near-complete restoration of the T lymphocyte population and thus most effectively showing the high-dose treatment.

It was observed that the level of recovery in CD4 marker expression in the standard treated group, **Fig 9H** was also very prominent and was comparative to the SBC Medium and high-treated groups. The structure expressed itself to be healthy with a considerable number of CD4+ cells, thus proving that the standard treatment restored the T lymphocyte population in the thymus tissue.

The results in thymic immunohistochemistry show a very definite gradient of recovery in the expression levels of CD4 markers in the treated groups. Indeed, though there was a drastic decline in populations of T-lymphocytes for the toxic control group, various treatments, especially at medium and high dose levels, showed a significant improvement in CD4 marker expression, thus signifying restorative immune function in the thymus.

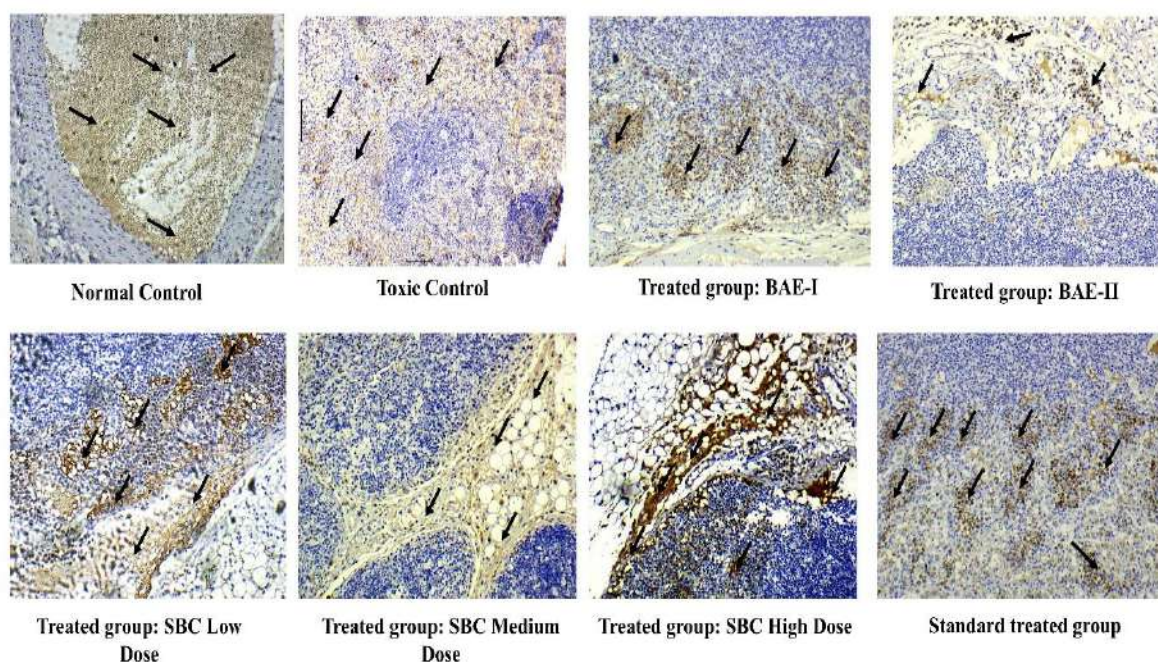


**Fig 9: Immunohistopathological examination of the transverse section of Spleen post-treating with CD4-antibodies. Where the moving arrows signify the produced lymphocytes. Where, 9A: Normal Control; 9B: Toxic control; 9C: Treated group (BAE-I); 9D: Treated group (BAE-II); 9E: Treated group (SBC Low dose); 9F: Treated group (SBC Medium dose); 9G: Treated group (SBC High dose) and 9H: Standard control**

#### **Impact of the research in the advancement of knowledge or benefit to mankind**

The study is useful for developing novel herbal alternatives against MAP infection for combating MAP-associated autoimmune disorders in human beings along with the additional immunomodulatory effect. The prepared extracts were standardized along with the scientific validation of their therapeutic potential against *Mycobacterium avium* subspecies *paratuberculosis*, becoming a solution to Antibiotic Multi-drug Resistance (AMR) to combat incurable Johne's disease of domestic livestock as well as for Crohn's disease in the human population. A synergistic combination has been developed and formulated into tablets for human beings and pills for ruminants.

#### **References**

- Anonymous 2001. The Ayurvedic Pharmacopoeia of India. 1<sup>st</sup> edition, Part-I, Vol-I. Govt. of India: Ministry of Health and Family Welfare, 123.
- Anonymous 2001a. The Ayurvedic Pharmacopoeia of India. 1<sup>st</sup> edition, Part-I, Vol-I. Govt. of

- India: Ministry of Health and Family Welfare, 59.
- Anonymous 1999. The Ayurvedic Pharmacopoeia of India. 1<sup>st</sup> edition, Part-I, Vol-II. Govt. of India: Ministry of Health and Family Welfare, 162.
- Anonymous 2001b. The Ayurvedic Pharmacopoeia of India. 1<sup>st</sup> edition, Part-I, Vol-I. Govt. of India: Ministry of Health and Family Welfare, 14.
- Anonymous 2004. The Ayurvedic Pharmacopoeia of India. 1<sup>st</sup> edition, Part-I, Vol-IV. Govt. of India: Ministry of Health and Family Welfare, 91.
- Anonymous, 2010. The Ayurvedic Pharmacopoeia of India, Part-I, Volume-I, in: The Ayurvedic Pharmacopoeia of India.
- Azagra-Boronat, I., Tres, A., Massot-Cladera, M., Franch, À., Castell, M., Guardiola, F., Pérez-Cano, F.J., Rodríguez-Lagunas, M.J., 2020. Associations of breast milk microbiota, immune factors, and fatty acids in the rat mother–offspring pair. *Nutrients*. <https://doi.org/10.3390/nu12020319>
- Fecteau, M.E., 2018. Paratuberculosis in Cattle. *Vet. Clin. North Am. - Food Anim. Pract.* <https://doi.org/10.1016/j.cvfa.2017.10.011>
- Gallo, L., Ramírez-Rigo, M.V., Piña, J., Palma, S., Allemandi, D., Bucalá, V., 2012. Valeriana officinalis dry plant extract for direct compression: Preparation and characterization. *Sci. Pharm.* <https://doi.org/10.3797/scipharm.1206-05>
- Goel, A., Singh, D.K., Kumar, S., Bhatia, A.K., 2010. Immunomodulating property of *Ocimum sanctum* by regulating the IL-2 production and its mRNA expression using rat's splenocytes. *Asian Pac. J. Trop. Med.* [https://doi.org/10.1016/S1995-7645\(10\)60021-1](https://doi.org/10.1016/S1995-7645(10)60021-1)
- Jayesh, K., Helen, L.R., Vysakh, A., Binil, E., Latha, M.S., 2017. In vivo toxicity evaluation of aqueous acetone extract of *Terminalia bellirica* (Gaertn.) Roxb. fruit. *Regul. Toxicol. Pharmacol.* <https://doi.org/10.1016/j.yrtph.2017.04.002>
- Kajaria, D., Tripathi, J., Tiwari, S., Pandey, B., 2013. Immunomodulatory effect of ethanolic extract of Shirishadi compound. *AYU (An Int. Q. J. Res. Ayurveda)*. <https://doi.org/10.4103/0974-8520.123136>
- Khan, W., Chester, K., Anjum, V., Ahmad, W., Ahmad, S., Narwaria, A., Prasanta, D., Katiyar, C.K., 2017. Phytochemistry Letters Chromatographic profiling of Pancharishta at different stages of its development using HPTLC, HPLC, GC – MS and UPLC – MS. <https://doi.org/10.1016/j.phytol.2017.04.034>
- Navabharath, M., Srivastava, V., Gupta, S., Singh, S.V., Ahmad, S., 2023. Ursolic Acid and Solasodine as Potent Anti-Mycobacterial Agents for Combating Paratuberculosis: An Anti-Inflammatory and In Silico Analysis. *Molecules*.



<https://doi.org/10.3390/molecules28010274>

- Nawaz, H., Shad, M.A., Rehman, N., Andaleeb, H., Ullah, N., 2020. Effect of solvent polarity on extraction yield and antioxidant properties of phytochemicals from bean (*Phaseolus vulgaris*) seeds. *Brazilian J. Pharm. Sci.* <https://doi.org/10.1590/s2175-97902019000417129>
- Parveen, A., Zahiruddin, S., Agarwal, N., Akhtar Siddiqui, M., Husain Ansari, S., Ahmad, S., 2021. Modulating effects of the synergistic combination of extracts of herbal drugs on cyclophosphamide-induced immunosuppressed mice. *Saudi J. Biol. Sci.* <https://doi.org/10.1016/j.sjbs.2021.06.076>
- Patwardhan, B., Mashelkar, R.A., 2009. Traditional medicine-inspired approaches to drug discovery: can Ayurveda show the way forward? *Drug Discov. Today.* <https://doi.org/10.1016/j.drudis.2009.05.009>
- Schena, E., Nedialkova, L., Borroni, E., Battaglia, S., Cabibbe, A.M., Niemann, S., Utpatel, C., Merker, M., Trovato, A., Hofmann-Thiel, S., Hoffmann, H., Cirillo, D.M., 2016. Delamanid susceptibility testing of *Mycobacterium tuberculosis* using the resazurin microtitre assay and the BACTEC™ MGIT™ 960 system. *J. Antimicrob. Chemother.* <https://doi.org/10.1093/jac/dkw044>
- Srivastava, V., Navabharath, M., Gupta, S., Singh, S.V., Ahmad, S., 2022. Exploration of *Solanum xanthocarpum* Schrad. & Wendl. against *Mycobacterium avium* Subspecies paratuberculosis and Assessment of Its Immunomodulatory and Anti-Inflammatory Potential. *Pharmaceuticals.* <https://doi.org/10.3390/ph15111367>
- Van Vuuren, S., Viljoen, A., 2011. Plant-based antimicrobial studies methods and approaches to study the interaction between natural products. *Planta Med.* <https://doi.org/10.1055/s-0030-1250736>
- Zahiruddin, S., Khan, W., Nehra, R., Alam, M.J., Mallick, M.N., Parveen, R., 2016. Pharmacokinetics and comparative metabolic profiling of iridoid enrich fraction of *Picrorhiza kurroa* - An Ayurvedic Herb. *J. Ethnopharmacol.*